Probabilistic Analysis of PV Generation Impacts on Voltage Sags in LV Distribution Networks Considering Failure Rates Dependent on Feeder Loading

João Eduardo Ribeiro Baptista ⬤, Anselmo Barbosa Rodrigues, and Maria da Guia da Silva ⬤, *Senior Member, IEEE*

Abstract—**The impact of photovoltaic distributed generation (PVDG) in the voltage sag indices of low-voltage distribution systems is assessed in this paper. A sensitivity study of these indices in relation to the penetration level of PVDG is performed considering the effect of the feeder sections loading on their failure rates. It is showed that, when this dependence is neglected, the indices are predicted with errors, especially for scenarios with large integration of PVDG. This study was performed using clustering techniques to model the uncertainty of solar irradiation, and the state enumeration method (SEM) is used to evaluate voltage sags indices. The results obtained by the clustering method and SEM were compared with those obtained with Monte Carlo Simulation based on the beta probability density function (pdf) model for solar irradiation. This comparison showed that the clustering model can obtain indices with precision comparable to those obtained with the beta pdf model, but with a significant reduction in CPU time.**

Index Terms—**Clustering methods, distributed power generation, distribution system planning, photovoltaic systems, power distribution, power quality, probabilistic techniques, solar power generation, voltage sags.**

NOMENCLATURE

A. Abbreviations

DG	Distributed generation.
DS	Distribution system.
LV	Low voltage.
LVDS	Low voltage distribution system.
MPPT	Maximum power point tracking.
PVA	Photovoltaic array.
PVC	Photovoltaic cell.
PVDG	Photovoltaic distributed generation.
PVP	Photovoltaic panel.
PVS	Photovoltaic string.

B. Variables[1]

I_{pv}, I_0	PVP's generated, and diode reverse saturation currents, respectively.
$I_{out}^{arr}, V_{out}^{arr}$	PVA's output current and voltage, respectively.
G, T	Incident irradiance (W/m^2) and PVC's junction temperature $(°K)$.

C. Parameters[1]

N_s, N_{ser}, N_{par}	Respectively, the numbers of: PVCs in series in a PVP, PVPs in series in a PVS and PVSs in parallel in a PVA.
R_s, R_p	Respectively, the equivalent series and parallel resistances of a PVP.
$I_{pv,n}$	PVP's generated current at nominal ambiance conditions: $G_n = 1000\,Wm^2$ and $T_n = 25\,°C\,(298{,}15\,°K)$.
a, K_I, K_V	Respectively, the PVP's diode ideality constant, and the current temperature (A/K) and voltage temperature (V/K) coefficients.
k, q	Respectively, the Boltzmann constant $(1.380\,6503 \times 10^{-23}\,J/K)$ and the elementary charge of the electron $(1.60217646 \times 10^{-19}\,C)$.

I. INTRODUCTION

THE installation of grid-tied PVDG has emerged as a profitable investment for DSs costumers all over the world, especially in countries with favorable irradiation indices and regulatory framework. In this way, a large growth in the penetration of PVDG in DSs is expected in the coming years, especially in LV systems, where PVDGs are more competitive than other types of DG. Because of this, the assessment of the impacts of the integration of PVDG into DSs is a research trend in power systems. Consequently, several papers have been published on the analysis of the effect of PVDG connection on the power quality indices, for example: long term voltage variations [1], voltage unbalance [2] and harmonics [3].

Voltage sag is the power quality disturbance that most often causes sensitive loads to trip [4]. This fact has motivated the

[1]All the currents are in Ampres and all the voltages are in Volts.

development of studies to estimate voltage sag indices [5]–[7] and to identify areas vulnerable to this disturbance [8].

However, the impacts of PVDG penetration on Voltage Sag Indices (VSI) of LVDSs has not yet been fully understood. The study in [9] performs the first attempt to assess this impact, but simplifies the method by considering only the output variability of the PVDGs rather than modeling that output as a function of a stochastic input irradiance (neglecting the internal model of the PVDGs plant), not modeling fault resistance variability and fault types different from the single line to ground (SLG) type, and by neglecting the protection response and thus the impact of PVDGs in the sags durations. In addition, the method in [9] does not consider the failure rates of the grid components, and therefore, can only predict the magnitude of the voltage sags, but can not predict the expected number of occurrences of these events.

There are two direct ways in which a DG plant can affect the voltage sags occurrence and severity: due to changes in the pre-fault voltage profile or due to its fault current contribution. Thus, both pre-fault and post-fault states should be considered in this type of study. In addition, the integration of PVDG can considerably change the loading condition of the distribution feeders, which is closely related to their failure rates [10]–[11]. Because of this, VSI can be affected by changing the failure rates of components caused by variations in the feeder sections loadings. However, even though loading condition dependent failure rates had already been modeled in reliability studies, until now, it was never considered in VSI assessment studies

The main aim of this paper is to perform a probabilistic assessment of the impact of the PVDG insertion on the VSI in LVDSs. The probabilistic method used to estimate VSI is the SEM proposed in [7]. This choice is due to SEM to be as precise as the MCS but considerably faster, because it needs fewer states to estimate the VSI [7]. The SEM was used to model uncertainties in the fault scenarios related to: short-circuit type (single-phase, two-phase, three-phase, etc.), fault position, faulted phases and solar irradiation. The solar radiation model in SEM is based on clustering techniques. The voltage sags resulting from uncertainties are evaluated using an expanded version of the Admittance Summation Method (ASM) [5], [7], [12] to model LVDSs with 4-wires. In addition, VSI are evaluated considering the effect of feeder loading on equipment failure rates due to PVDG integration. The tests results with the CIGRÈ European Low Voltage Test System (CELVTS) [13] show that the predicted voltage sag indices may be imprecise for high levels of PVDG penetration when the dependence of the failure rate in relation to the feeder loading is neglected. In addition, it was demonstrated that the VSI calculated by the SEM, with PVDG modeled using clustering techniques, has acceptable accuracy and low computational cost over those evaluated by MCS, with PVDG modeled via beta distribution.

In this way, the main contributions and innovations of this paper are:

i) Expansion of the ASM for applications in fault analysis of LVDSs with 4-wires;

ii) Modeling of PVDG in short circuit calculations for VSI estimation;

iii) Modeling of uncertainties related to solar irradiation based on clustering techniques for probabilistic VSI estimation;

iv) Computation of VSI considering failure rates as function of feeder loading.

v) Introduction of a new SEM for fast and accurate VSI estimation in distribution networks with high penetration of PVDG.

vi) Considering the effect of PVDGs in sags time durations due to its interaction with the systems protection.

II. FAULT ANALYSIS IN LV 4-WIRED SYSTEMS

In this paper, a 4-wire version of phase coordinate ASM is used to evaluate the system voltages and currents during a fault in LVDSs using the technique proposed in [5]. This new version of ASM preserves all the backward/forward sweep equations of the original ASM proposed in [12], including the equations relative to the branches of the transformer type. The next subsections present the 4-wires models for the main components of low voltage DSs.

A. Network Components Modeling in the 4-Wire ASM

1) Loads and Neutral Grounding Modeling: Consider the polinomial load model, where the complex load connected to a given phase ϕ at node k is noted as:

$$P_k^\phi + jQ_k^\phi = P_{0_k}^\phi \left(\alpha_{p_k}^\phi + \beta_{p_k}^\phi V_k^{\phi n} + \gamma_{p_k}^\phi V_k^{\phi n\,2} \right) + jQ_{0_k}^\phi \left(\alpha_{q_k}^\phi + \beta_{q_k}^\phi V_k^{\phi n} + \gamma_{q_k}^\phi V_k^{\phi n\,2} \right) \quad (1)$$

Where:
$P_k^\phi (Q_k^\phi)$ is the active (reactive) power of the load.
$P_{0_k}^\phi (Q_{0_k}^\phi)$ is the active (reactive) rated power of the load.
$\alpha_{p_k}^\phi, \beta_{p_k}^\phi, \gamma_{p_k}^\phi, \alpha_{q_k}^\phi, \beta_{q_k}^\phi \text{ and } \gamma_{q_k}^\phi$ are load type partition factors, i.e., $\alpha_{p_k}^\phi + \beta_{p_k}^\phi + \gamma_{p_k}^\phi = \alpha_{q_k}^\phi + \beta_{q_k}^\phi + \gamma_{q_k}^\phi = 100\,\%$.
$V_k^{\phi n}$ is the magnitude of the voltage between phase ϕ and neutral wire at node k, given by:

$$V_k^{\phi n} = \left| E_k^{\phi n} \right| = \left| E_k^\phi - E_k^n \right| \quad (2)$$

Where $E_k^{\phi n}$, E_k^ϕ and E_k^n are, respectively, the complex voltages at node k between phase ϕ and neutral wire, between phase ϕ and the reference, and between the neutral wire and the reference.

In ASM the constant impedance loads are modeled as shunt admittances and the constant power and constant current loads are modeled as equivalent current injections as:

$$y_k^\phi = \gamma_{p_k}^\phi P_{0_k}^\phi - j\gamma_{q_k}^\phi Q_{0_k}^\phi \quad (3)$$

$$I_k^\phi = \frac{P_{0_k}^\phi \left(\alpha_{p_k}^\phi + \beta_{p_k}^\phi V_k^{\phi n} \right) - jQ_{0_k}^\phi \left(\alpha_{q_k}^\phi + \beta_{q_k}^\phi V_k^{\phi n} \right)}{\left(E_k^{\phi n} \right)^*} \quad (4)$$

Where y_k^ϕ is the equivalent admittance for the loads modeled as constant impedance and I_k^ϕ is the equivalent current injection for the loads modeled as constant current and constant power.

After finding the load equivalents per phase, the 4-wire models in the node k of the constant impedance type loads YL_k and the current equivalent injections related to the constant current and constant power type loads JL_k, respectively, can be obtained as (5) and (6) where y_k^g is the neutral grounding admittance at node k.

$$YL_k = \begin{bmatrix} y_k^a & 0 & 0 & -y_k^a \\ 0 & y_k^b & 0 & -y_k^b \\ 0 & 0 & y_k^c & -y_k^c \\ -y_k^a & -y_k^b & -y_k^c & y_k^a + y_k^b + y_k^c + y_k^g \end{bmatrix} \quad (5)$$

$$JL_k = \begin{bmatrix} I_k^a & I_k^b & I_k^c & -\left(I_k^a + I_k^b + I_k^c\right) \end{bmatrix}^T \quad (6)$$

2) Transformer Modeling: The transformers equations for phase coordinate ASM, proposed in [12], are based on their admittance matrix (Y_t). A 3-wire model of these matrices has been evaluated for most types of transformers in [14]. The same method is used in this paper to obtain the 4-wire model of a $\Delta - Y$ grounded transformer showed in (7).

$$Y_t = y_t \begin{bmatrix} \frac{2}{3} & -\frac{1}{3} & -\frac{1}{3} & 0 & -\frac{1}{\sqrt{3}} & 0 & \frac{1}{\sqrt{3}} & 0 \\ -\frac{1}{3} & \frac{2}{3} & -\frac{1}{3} & 0 & \frac{1}{\sqrt{3}} & -\frac{1}{\sqrt{3}} & 0 & 0 \\ -\frac{1}{3} & -\frac{1}{3} & \frac{2}{3} & 0 & 0 & \frac{1}{\sqrt{3}} & -\frac{1}{\sqrt{3}} & 0 \\ 0 & 0 & 0 & 0 & 0 & 0 & 0 & 0 \\ -\frac{1}{\sqrt{3}} & 0 & \frac{1}{\sqrt{3}} & 0 & 1 & 0 & 0 & -1 \\ \frac{1}{\sqrt{3}} & -\frac{1}{\sqrt{3}} & 0 & 0 & 0 & 1 & 0 & -1 \\ 0 & \frac{1}{\sqrt{3}} & -\frac{1}{\sqrt{3}} & 0 & 0 & 0 & 1 & -1 \\ 0 & 0 & 0 & 0 & -1 & -1 & -1 & 3+\frac{y_g}{y_t} \end{bmatrix} \quad (7)$$

Where y_t and y_g are, respectively, the transformer and the grounding admittances.

III. VOLTAGE SAG CHARACTERIZATION

Voltage sags are temporary reduction in the Root Mean Square (RMS) value of the supply voltage to a value between 0.1 p.u. and 0.9 p.u. with duration between 0.5 cycle and 1 minute. To assess the performance of the systems in relation to voltage sags, some RMS variation indices are proposed in the literature, the most popular being the $SARFI_x$ indices [4]. These indices are usually weighted by the number of customers in each load point affected by the sags. In the absence of the number of customers, the weights of the $SARFI_x$ index can be based on the load point kVA. Thus, the $SARFI_x$ index can be defined as:

$$SARFI_{x\%} = \frac{\sum_{i=1}^{NSN} NS_i^{x\%} \times S_i}{\sum_{i=1}^{NSN} S_i} \quad (8)$$
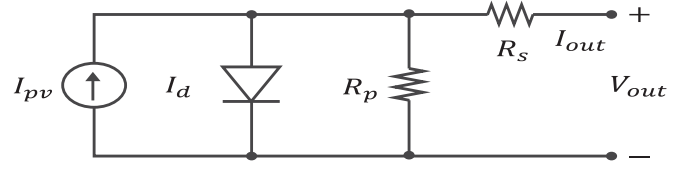

Fig. 1.   Equivalent circuit of a PVP.

Where NS_i^x is the number of sags in the study period with post fault voltages below the threshold x % at node i, S_i is the apparent rated power at node i and NSN is the number of load points in the system. In addition, the threshold x can be replaced by an experimental Voltage Tolerance Curve (VTC). In this way, the SARFI index considers sags with magnitude and duration characteristics that probably can trip sensitive loads. For example, the $SARFI_{SEMI}$ takes into account the voltage sags that violate the SEMI 47 VTC [15]. In this paper, the threshold values used for x are: 90%, 80%, 70%, 50% and the SEMI curve.

IV. PROBABILISTIC MODELING OF PVDG SYSTEMS

A. PVDG Models in the Pre-Fault and Post-Fault States

A typical grid-tied PVDG plant is composed of an inverter delivering power to the grid, supplied by a PVA of series/parallel PVPs. To model the behavior of PVPs, the circuit showed in Fig. 1 is used. Considering this circuit and the PVPs' series/parallel associations, the output current (I_{out}^{arr}) and the output voltage (V_{out}^{arr}) of the PVA are related in (9)–(13) [1].

$$I_{out}^{arr} = I_{pv} N_{par} - I_0 N_{par} \left[\exp(\delta) - 1\right] - I_{R_p}^{arr} \quad (9)$$

$$I_{R_p}^{arr} = \frac{V_{out}^{arr} + R_s \left(N_{ser}/N_{par}\right) I_{out}^{arr}}{R_p N_{ser}/N_{par}} \quad (10)$$

$$\delta = \frac{V_{out}^{arr} + R_s \left(N_{ser}/N_{par}\right) I_{out}^{arr}}{aV_t N_{ser}} \quad (11)$$

$$I_{pv} = \left(I_{pv,n} + K_I \Delta_T\right) G/G_n \quad (12)$$

$$I_0 = \frac{I_{pv,n} + K_I \Delta_T}{\exp\left[\left(V_{oc,n} + K_V \Delta_T\right)/aV_T\right] - 1} \quad (13)$$

Where $V_t = N_s kT/q$ is the thermal voltage of the PVP, $V_{oc,n}$ is the open circuit voltage at nominal ambience conditions and $\Delta_T = T - T_n$. The substitution of (10)–(13) into (9) results in a transcendental equation only solvable by numeric methods.

The operating point $(I_{out}^{arr}, V_{out}^{arr})$ of the PVA is controlled by the inverter with a MPPT strategy. This control aims to deliver the maximum possible power from a given pair of inputs (G, T). The output power P_{out}^{arr} of the PVA can be find by simulating this control using the algorithm in Fig. 2, a sequential search of the maximum power point (MPP) by initiating the voltage at 0 V and increasing it by increments of 1% of the open circuit voltage. In each step, the MPP is updated if the power increases with voltage, otherwise the algorithm stops.

After obtaining P_{out}^{arr}, the power delivered to the grid by the inverter P_{out}^{inv} is obtained by (14) [1], where η_{inv}, η_m, η_d are efficiency factors that model the losses related to the inverter,
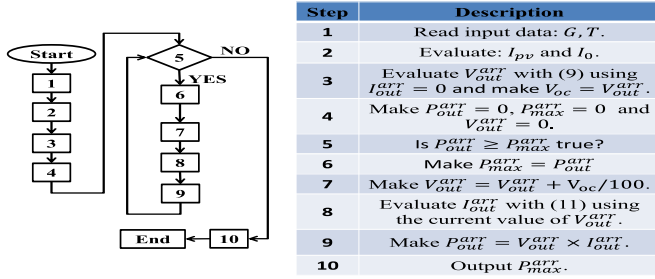
Step	Description
1	Read input data: G, T.
2	Evaluate: I_{pv} and I_0.
3	Evaluate V_{out}^{arr} with (9) using $I_{out}^{arr} = 0$ and make $V_{oc} = V_{out}^{arr}$.
4	Make $P_{out}^{arr} = 0$, $P_{max}^{arr} = 0$ and $V_{out}^{arr} = 0$.
5	Is $P_{out}^{arr} \geq P_{max}^{arr}$ true?
6	Make $P_{max}^{arr} = P_{out}^{arr}$
7	Make $V_{out}^{arr} = V_{out}^{arr} + V_{oc}/100$.
8	Evaluate I_{out}^{arr} with (11) using the current value of V_{out}^{arr}.
9	Make $P_{out}^{arr} = V_{out}^{arr} \times I_{out}^{arr}$.
10	Output P_{max}^{arr}.

Fig. 2. Flowchart of the MPPT simulation algorithm.

TABLE I
CLUSTERING ANALYSIS OF THE IRRADIANCE DATA

Cluster	G (W/m²)	Nº of elements	Probability (%)
1	0.0000	258459	49.1741
2	264.683	66697	12.6897
3	468.267	49717	9.4591
4	971.098	35449	6.7445
5	712.626	38595	7.3430
6	66.022	76683	14.5896
Total		**525600**	**100**

incompatibility between PVPs, and dirt coverage on PVPs surfaces, respectively.

$$P_{out}^{inv} = \eta_{inv} \times \eta_m \times \eta_d \times P_{out}^{arr} \quad (14)$$

Finally, in order to find the current injections of PVDG in the pre-fault and post-fault states, some controls must be considered. The PVDG's inverter usually controls the current injection to operate at a constant unitary power factor, providing only active power to the grid [16]. In addition, for three-phase inverters, only perfectly balanced currents are injected into the grid, even when they experience unbalanced voltage conditions, injecting only positive sequence currents [17]. Therefore, the positive sequence current of phase a (I_+), injected by a three-phase inverter is given by (15), where E_+ is the positive sequence voltage of phase a.

$$I_+ = P_{out}^{inv} / E_+ \quad (15)$$

In the case of a single phase inverter, which is a common case for low capacity PVDGs, only the unitary power factor control must be considered, and the injected current in phase ϕ (I_ϕ) is given by (16), in which E_ϕ is the voltage in phase ϕ.

$$I_\phi = P_{out}^{inv} / E_\phi \quad (16)$$

In the event of a fault in the system, the PVDGs will contribute to the fault current. Since protection tends to eliminate faults in a short time (usually from 0.5 cycle to a few seconds in DSs [18]), the irradiance fluctuations during the fault can be neglected and the PVDGs contribution can be evaluated for a constant irradiance. According to [17], due to the MPPT control, for a given irradiance, the PVDG will behave as an independent power source, thus constant regarding the voltage. However, the current contribution of PVDGs is limited to a maximum magnitude by the inverter. Therefore, if this threshold is reached, the PVDG starts to behave as a current source with a constant magnitude and a voltage dependent angle. Therefore, the fault current contributions of a three-phase and single phase PVDGs are given, respectively, by (17) and (18).

$$\begin{cases} I_+^{Fault} = I_+, & if \ I_+ < I_{\max} \\ I_+^{Fault} = I_{\max} \angle \theta_{E_+} & if \ I_+ \geq I_{\max} \end{cases} \quad (17)$$

$$\begin{cases} I_\phi^{Fault} = I_\phi, & if \ I_\phi < I_{\max} \\ I_\phi^{Fault} = I_{\max} \angle \theta_{E_\phi} & if \ I_\phi \geq I_{\max} \end{cases} \quad (18)$$

Where I_+^{Fault} (I_ϕ^{Fault}) is the contribution of positive sequence (phase ϕ) fault current of a three-phase (single-phase) PVDG, $I_{\max}$ is the maximum fault contribution current magnitude of the PVDG's inverter and θ_{E_+} (θ_{E_ϕ}) is the angle of positive sequence (phase ϕ) voltage at the PVDG's node.

B. Probabilistic Modeling of the Irradiance Input

1) Modeling the Irradiance Uncertainty in the SEM: The simplifications required by the SEM to obtain discrete random variables can be done in two ways: by discretizing the PDFs of the variables or by clustering historical data related to them. In this work, the clustering approach was chosen to model irradiance uncertainty due to its simplicity and reduced number of states compared to the PDF discretization approach, as will be demonstrated. The k-means algorithm was applied to a database composed of 525,600 measurements collected from the São Luís station of the SONDA's project [19] in Brazil's Northeast for 1 year with a sample rate of 1 minute. These data were grouped in 6 clusters showed in Table I, being one of the clusters reserved to zero values of irradiance.

Once the irradiance states are defined, the power output of the PVDGs in each state can also be preprocessed to create two input files: one with the power output of the PVDGs in each state, and one that relates the states to their probabilities. This disassociates this evaluation from the main algorithm, which may be useful to reduce computational effort by conducting multiple studies using the same PVDG allocation, e.g., when considering different scenarios of expansion planning.

2) Modeling the Irradiance Uncertainty in MCS: In this paper MCS is used only with the intention of validating the proposed SEM. Therefore, the irradiance uncertainty model used with this method aims at high accuracy without considering the impacts on the computational effort of the method. The model proposed in [20] was selected to model solar irradiance in MCS. This model consists of generating typical days for each season of the year. Then a Beta PDF is adjusted for each hourly interval of those days (except for the night hours that are adjusted to 0 W/m²) considering the hourly fluctuations of the irradiance. The Beta PDF is defined in (19).

$$f_b(g) = \frac{\Gamma(\alpha + \beta)}{\Gamma(\alpha) \times \Gamma(\beta)} \times g^{(\alpha - 1)} \times (1 - g)^{(\beta - 1)} \quad (19)$$

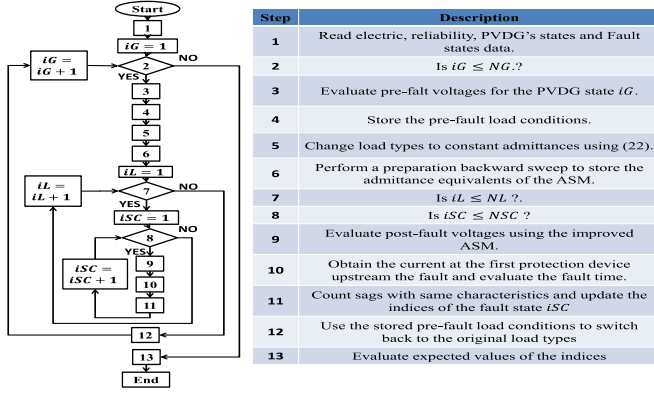Where Γ is the Gamma function, g is the irradiance normalized by the maximum value G_{peak} in the sample space,

Fig. 3. Flowchart of the SEM for voltage sag analysis considering PVDG.

Step	Description
1	Read electric, reliability, PVDG's states and Fault states data.
2	Is $iG \leq NG$.?
3	Evaluate pre-falt voltages for the PVDG state iG.
4	Store the pre-fault load conditions.
5	Change load types to constant admittances using (22).
6	Perform a preparation backward sweep to store the admittance equivalents of the ASM.
7	Is $iL \leq NL$?.
8	Is $iSC \leq NSC$?
9	Evaluate post-fault voltages using the improved ASM.
10	Obtain the current at the first protection device upstream the fault and evaluate the fault time.
11	Count sags with same characteristics and update the indices of the fault state iSC
12	Use the stored pre-fault load conditions to switch back to the original load types
13	Evaluate expected values of the indices

therefore $0 \leq g \leq 1$, and α and β are the PDF parameters, which must satisfy $\alpha \geq 0$ and $\beta \geq 0$. The PDF parameters can be found using the mean μ and the variance σ^2 of the samples as:

$$\beta = (1 - \mu) \times \left(\frac{\mu \times (1 + \mu)}{\sigma^2} - 1 \right) \tag{20}$$

$$\alpha = \frac{\mu \times \beta}{1 - \mu} \tag{21}$$

The irradiance database used to generate the PDFs was also obtained from the São Luís station of the SONDA project [19]. However, a second year of measurements was also included, doubling the number of samples in order to gain a higher level of confidence. The first step in applying the methodology described in this section is to evaluate the mean values of the measurements for each hour considering a sample of 60 minutes for each hour. Then, according to the local climate, the hourly measurements were grouped into two seasons: rainy (January to June) and dry (July to December). All hourly average irradiances belonging to the same season of the year are grouped and normalized by the maximum value in each group. Finally, the Beta PDF's parameters are obtained for each hour of the day of the typical season, which, according to the measurements, occurs from 5 a.m. to 7 p.m. It should be noted that this methodology produces 24 different PDFs, which is why a PDF discretization approach would produce a large number of states, reducing the efficiency of SEM.

V. PROPOSED METHOD OF VOLTAGE SAG ASSESSMENT USING SEM

The SEM is a simple, but powerful tool to assess the expected values of the voltage sag indices. The study in [7] used this method to evaluate indices in a primary distribution system considering uncertainties related to fault resistance, fault position, type of fault and the set of phases involved in a fault. In this paper, the SEM is expanded to consider the uncertainty of the PVDGs output power. The flowchart of the proposed method is showed in Fig. 3.

In fault studies, loads are generally modeled as constant admittances [21]. Therefore, in step 5 of Fig. 3, loads are changed

to this type using (22).

$$y_k^\phi = \left(P_k^\phi - jQ_k^\phi \right) \Big/ \left(V_k^{\phi n} \right)^2 \tag{22}$$

Since this conversion is dependent of the pre-fault state, the use of the improved ASM proposed in [7] is limited to faults occurring in the same pre-fault state. This requires a backward sweep preparation for each irradiation state. However, reducing CPU effort in subsequent fault evaluations easily compensates for these additional sweeps.

Using the algorithm proposed in Fig. 3, the $SARFI_{x\%}$ indices are evaluated as in (23).

$$SARFI_{x\%} = \frac{\sum_{iL=1}^{NL} \sum_{iF=1}^{NF} S_x^{tot}(iL, iF) \, P(iG) \, P(iF) \, \lambda_{iL}}{\sum_{iB=1}^{NB} S_{iB}} \tag{23}$$

Where λ_{iL} is the failure rate of the feeder section i_L, $P(iG)$ is the probability of the pre-fault state iG, $P(iF)$ is the probability of the fault state iF, NL is the number of feeders sections in the system, NF is the number of fault states, NB is the number of buses, S_m is the load kVA at bus iB and $S_x^{tot}(iL, IF)$ is the total apparent power affected by a voltage sag under the threshold x %, evaluated by (24) and (25).

$$S_x^{tot}(iL, iF) = \sum_{iB=1}^{NB} u(iL, iF) \times S_{iB} \tag{24}$$

$$u(iL, iF) = \begin{cases} 1, & V_{iB}^{\phi n}(iL, iF) \leq x \% \\ 0, & otherwise \end{cases} \tag{25}$$

Where $V_{iB}^{\phi n}(iL, iF)$ is the voltage between the phase ϕ and the neutral wire at the node iB for a given fault in the branch iL with parameters given by the fault state iF, which, in this paper, is composed of a combination of the following random variables states: position (P_{iF}), impedance (Z_{iF}), type (T_{iF}) and the set of phases involved in a fault (Ph_{iF}). Thus, the probability of iF is given by $P(iF) = P(P_{IF}) \times P(Z_{If}) \times P(T_{iF}) \times P(Ph_{iF})$. The modeling of the uncertainty of these variables is identical to [7].

VI. A MCS APPROACH FOR BENCHMARKING PURPOSES

The flowchart of the MCS algorithm used to validate the results obtained by SEM is showed in Fig. 4 where: NY is the maximum number of years to be simulated; iY is the year counter; NL is the number of feeder sections in the system; iL is a pointer to each section; NF is the number of faults sampled for a section and iF is a pointer for each fault of that respective section. The uncertainty models used for the fault scenario variables and the number of faults in a feeder section are the same as those used in [7] as well as the stopping criteria used in this MCS.

VII. FAILURE RATE MODEL OF DISTRIBUTION FEEDERS BASED ON LOADING CONDITION

Feeders failure rates are related to many factors. Some of them are independent of the operating conditions of the system, for
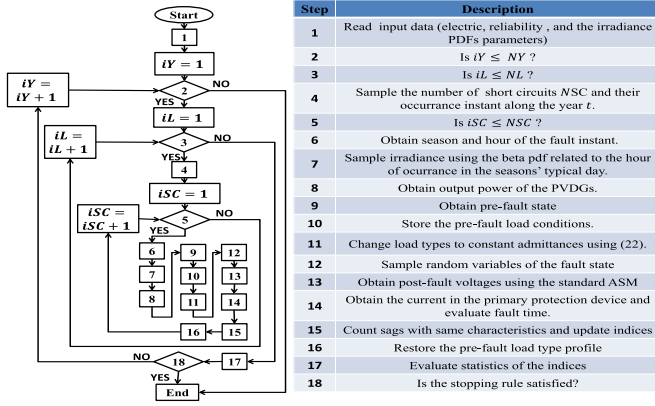
Fig. 4. Flowchart of the MCS used to validate the results of the SEM.

Fig. 5. SEM and MCS results for the 20% PVDG penetration case.

for $r(I_\%)$.

$$r\left(I_\%\right) = \frac{1}{1 + e^{-10\left(I_\%\ -0.5085\right)}} \qquad (27)$$

VIII. RESULTS

A. Description of the Test System and Study Cases

The methodology proposed in this paper was applied to the CELVTS [13]. In this system, fuses for residential, industrial and commercial feeders were considered 15 K, 6 K, and 10 K types respectively. These were sized to be the fastest fuses that could still withstand an inrush current 12 times higher than the transformers rated currents over a period of $0.1\ s$. To model the fuses, the data provided by the manufacturer's website were interpolated using cubic spline curves.

In the original CELVTS, the loads connected to the substation buses of the residential and commercial feeders are in fact equivalent to parallel feeders. These loads were excluded from the tests, since they are very high compared to the loads of other nodes, and have a better voltage support due to the proximity to the substation. These characteristics will certainly introduce bias in the indices.

The impact assessment of the penetration of PVDG in the $SARFI_{x\%}$ indices was performed using two models for failure rates: constant ($\lambda_p = 0.088\ faults/(year \times mile)$) [23] and loading dependent. For both models, it was considered that the temporary faults are 82.5% of the total number of faults [7] and the total failure rate is reached by proportion.

The failure rate models were assessed considering eleven case studies obtained by varying the percentage of PVDG penetration (in relation to total system load) from 0% to 200% in steps of 20%. It was also considered that all load points have PVDG systems with capacity proportional to the penetration level considered in the case study. All tests using SEM considered 1 fault position, 5 fault resistance states and the same fault type probabilities of [7] to model the fault scenario. The irradiance uncertainty was modeled using the states of Table I. Finally, MCS and SEM were applied to the case study with 20% of PVDG penetration and condition dependent failure rates. This analysis was performed with the objective of comparing the computational cost and the accuracy of the SEM in relation to the MCS.

B. SEM Benchmarking Using MCS

The indices obtained by SEM and MCS are shown in Fig. 5. This figure clearly demonstrates that both methods achieved

example, exposure to adverse weather, vandalism, high density of vegetation, animals, etc. However, some causes of failure are related to the loading condition of the feeders. The heat power produced by active losses is proportional to the square of the current, and the high temperatures increases the risk of feeders failure in several ways, for example, reducing the mechanical strength of the wires due to annealing [11], increasing the risk of contact with underneath objects due to sagging [10], and degrading the dielectric material of cables and insulation chains [10].

Since the insertion of the distributed generation in the grid can change the average loading levels of the wires, it is important to consider the impacts of this change in failure rates, in order to fully assess the impacts of the PVDGs in the voltage sag indices. There are many models proposed in the literature to explain this correlation, for example, those presented in [10] and [11]. However, according to [22], the model that best describes this relationship is the function in (26).

$$\lambda_p\left(r\right) = Ae^{Br} + C \qquad (26)$$

Where: λ_p is the permanent failure rate; A, B and C are the parameters obtained in [23] from empirical data and r is a function that maps the condition score of the equipment to values in the interval [0, 1], where 0 and 1 are the values assigned to the best and the worst possible conditions, respectively.

In this paper, the constant parameters in (26) are made in the same as those obtained in [22], but several models were tested for the score condition r as a function of a feeder's loading percentage annual average $I_\%$. In order to obtain a realistic model, the following criteria were used:

- The function $r(I_\%)$ must be 0 when $I_\% = 0\%$.
- The function $r(I_\%)$ must be 1 when $I_\% \geq 100\%$.
- The average failure rate obtained for the system using (26) should be as close as possible to the empirical average failure rate given by [22].
- The curve obtained must be continuous and desired to be smooth.

The application of this methodology using data from the CIGRÈ European Low Voltage Test System (CELVTS) [14] indicated the function defined in (27) as the best candidate found
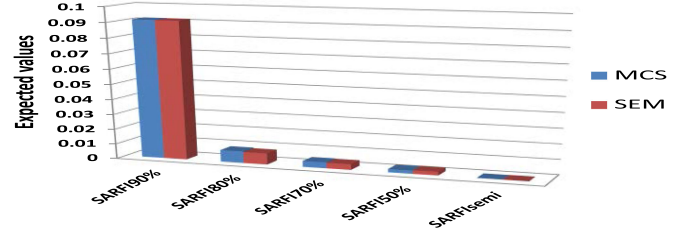
TABLE II
$SARFIs$ OF EACH PENETRATION (PEN ACRONYM IN THE UPPER LEFT CORNER) CASE USING THE CONSTANT λ MODEL

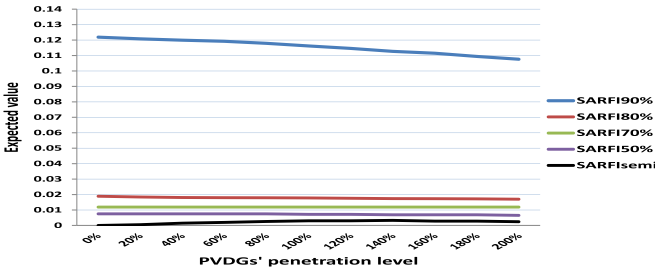| PEN	Index				
(%)	$SARFI_{90\%}$	$SARFI_{80\%}$	$SARFI_{70\%}$	$SARFI_{50\%}$	$SARFI_{SEMI}$
0	0.1219	0.0189	0.0119	0.0075	0.0000
20	0.1208	0.0184	0.0119	0.0075	0.0005
60	0.1199	0.0181	0.0119	0.0075	0.0015
40	0.1192	0.0180	0.0119	0.0075	0.0020
80	0.1179	0.0179	0.0119	0.0075	0.0026
100	0.1162	0.0178	0.0119	0.0072	0.0030
120	0.1146	0.0176	0.0119	0.0072	0.0030
140	0.1127	0.0174	0.0119	0.0069	0.0033
160	0.1115	0.0173	0.0119	0.0069	0.0028
180	0.1094	0.0172	0.0119	0.0069	0.0028
200	0.1076	0.0170	0.0119	0.0065	0.0024

TABLE III
$SARFIs$ OF EACH PENETRATION (PEN ACRONYM IN THE UPPER LEFT CORNER) CASE USING THE DEPENDENT λ MODEL

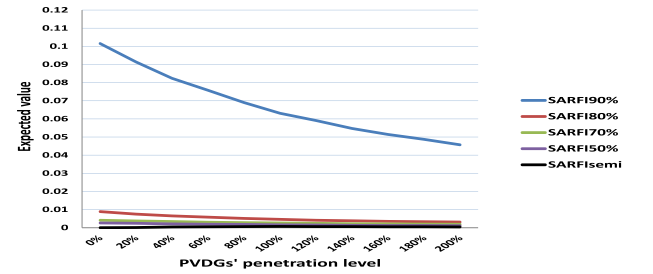| PEN	Index				
(%)	$SARFI_{90\%}$	$SARFI_{80\%}$	$SARFI_{70\%}$	$SARFI_{50\%}$	$SARFI_{SEMI}$
0	0.1016	0.0089	0.0041	0.0026	0.0000
20	0.0914	0.0075	0.0037	0.0024	0.0001
60	0.0824	0.0065	0.0034	0.0021	0.0004
40	0.0758	0.0058	0.0030	0.0019	0.0005
80	0.0690	0.0051	0.0028	0.0018	0.0006
100	0.0631	0.0046	0.0026	0.0016	0.0007
120	0.0591	0.0041	0.0024	0.0015	0.0006
140	0.0547	0.0038	0.0022	0.0013	0.0006
160	0.0514	0.0035	0.0021	0.0012	0.0005
180	0.0487	0.0033	0.0020	0.0012	0.0005
200	0.0457	0.0031	0.0019	0.0011	0.0004

Fig. 6. $SARFI$ indices regarding PVDG penetration (constant λ model).

Fig. 7. $SARFI$ indices regarding PVDG penetration (dependent λ model).

comparable precision. However, CPU times were considerably different. The MCS needed 11 h 53 min and 6 s to run, while the SEM run in only 2 min and 8 s. In other words, the SEM is approximately 333.18 times faster than the MCS.

C. Voltage Sag Indices Variation Due to PVDG Penetration

The results of the $SARFI_x$ indices of each PVDG penetration scenario assessed with the constant failure rate model are shown in Table II. There is a slightly decrease tendency of indices in relation to only the magnitudes of sags. The $SARFI_{SEMI}$, however, follows an increasing tendency of 0% to 100% penetration of PVDGs, after which it begins to decrease. These effects are explained by the contributions of the PVDGs to the fault current, which relieves system's loading during the fault, raising the voltage profile, but also reducing the fuse current and increasing its response time. Therefore, the growth or reduction of $SARFI_{SEMI}$ depended on which effect outperformed the other, in relation to the SEMI VTC.

Although the indices have varied with the growth of PVDG penetration, their variations are quite small, as can be seen in Fig. 6. Two facts explain this behavior. The first is the inverter limitation of the fault current contributions to a specified maximum value. The other, is the low probability of a fault to occur in a period of high irradiance, as these occurs only at specific times of the day, while a fault can occur at any time. Evidently, during low irradiance states, the available power output of PVDGs to contribute to the fault current is severely reduced.

Table III shows the variation of the $SARFI_x$ indices in relation to the penetration of PVDGs when the failure rates are obtained by (25). It can be seen that the magnitude of the in-

dices are greatly reduced as the penetration of PVDG increases, which can be seen in Fig. 7. In addition, the growing tendency of $SARFI_{SEMI}$, observed in the constant failure rate model, is much more limited in the condition based model since it is compensated by the reduction in the number of faults. These facts clearly demonstrate that the indirect effect of PVDGs in reducing failure rates by relieving feeders loading causes greater impact on voltage sag indices than the direct effect of contributing to fault currents.

Finally, a comparison between both models shows that neglecting variations in the failure rate due to loading changes leads to errors, even for the base case. $SARFI_{90\%}$ is overestimated at 19.98% when the constant failure rate is used to assess base case indices. These errors are even greater as the penetration of PVDG increases, e.g., the $SARFI_{90\%}$ is overestimated at 135.45% for the case of penetration of 200%.

IX. COMPARISON OF VSI ESTIMATION METHODS

The impact of PVDGs penetration regarding the VSI of a LVDS has also been recently analyzed in [9]. This method, which is described in Fig. 5 of the aforementioned reference, consists in performing an MCS study for each PVDG penetration level considered (the penetration level on that study is defined as the ratio between the number of load nodes with PVDG and the total number of load nodes). The allocation of the PVDGs in each penetration level is made by choosing the nodes using a random sampling with no replacement and the rated powers by using rectangular distribution from 1 kW up to 5 kW. Then, for each penetration level, MCS simulation is used to generate one hundred SLG fault states, considering

uncertainties in the fault position with regard to the nodes, faulted phase, PVDGs generated power output and load demand. This MCS is then used to obtain the cumulative distribution functions (CDFs) of the magnitude of the sags V_{sag} for each penetration level.

As already stated in the introduction, the aforementioned study has some considerable drawbacks when compared to the one in this paper because it only evaluates indices related to the sags magnitudes, neglecting their time durations and the expected number (frequency) of voltage sags. In this paper, it was shown that these aspects are very important to achieve a full comprehension on the PVDGs impacts on the voltage sag phenomenon.

The method proposed in [9] assumes some simplifications which compromises its precision: not modeling the internal behavior of the PVDGs plants, by using instead, a PVDGs output profile database; not modeling the fault resistance variability and, finally; considering only SLG faults. In order to show the impact of these simplifications, this section provides a comparative analysis this method for 3 cases:

i) *Case # 1:* the original assumptions are used.
ii) *Case # 2:* the models proposed in this paper are used.
iii) *Case # 3:* uses the proposed SEM instead of the MCS.

For these studies, some further assumptions were made. In case # 1, due to lack of information, it was assumed a constant fault resistance of 0 Ω, a regular 3-wire ASM was used for fault analysis, and since the PVDGs are not explicitly modeled, it was assumed that their current limits are neglected. In case # 2 the irradiance states were sampled from the data clusters shown in Table I, as it was already shown that this model is sufficiently precise. In addition, for all the cases, the loads of the fault states were modeled by constant admittances obtained from the pre-fault scenario using (22) and the pre-fault load variations were neglected. Finally, aiming for simplicity in cases # 2 and # 3, the power outputs at each irradiance state, and the maximum fault contribution currents of the allocated PVDGs were obtained by multiplying their rated capacity, respectively, by the power output and the maximum current of a reference 5 kW PVDG.

In order to obtain the CDFs of the voltage sag magnitudes using the SEM, the interval between 0 and 0.9 p. u. is subdivided in a large number of intervals and the expected number of sags within each of these intervals is obtained, generating a histogram from which the CDF can be found. The results obtained by the proposed study cases in each penetration level are show, respectively, in Fig. 8, Fig. 9 and Fig. 10.

By comparing the results, it becomes clear that the assumptions of case # 1 distorts the indices as sags seems more dispersed in a broad range of magnitudes when in reality they tend to concentrate between 0.8 and 0.9 per unit. The probable reason for this is that neglecting fault resistance favors sags with lower remaining voltages. Also, from Fig. 9 and Fig. 10 it can be seen that the SEM proposed in this paper is also perfectly capable of obtaining the CDFs of the sags remaining voltages. Finally, since the curves in Fig. 10 are so close that are superposing each other, it can be seen that the variability in Fig. 9 is actually due to random sampling of MCS (which is been interrupted after 100 states instead of using a convergence stopping criteria) and not
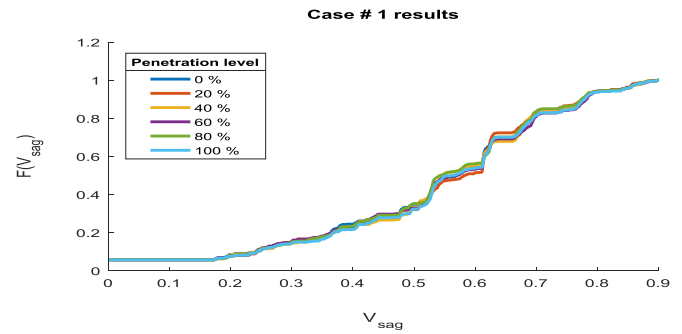

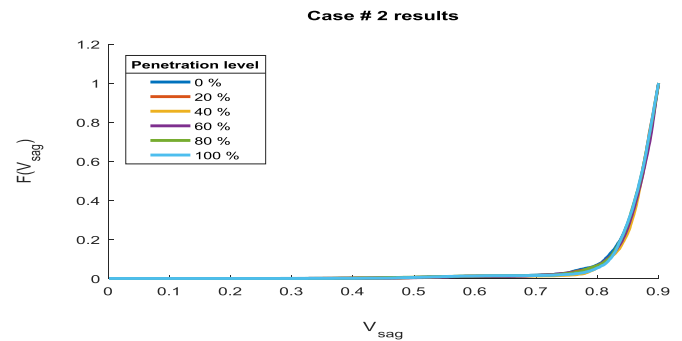Fig. 8. CDFs of V_{sag} for each penetration level of the case # 1.

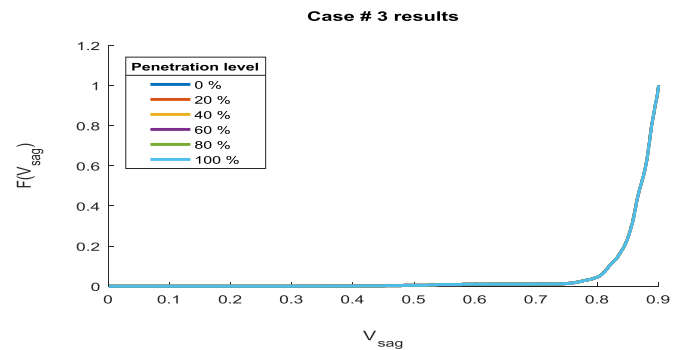Fig. 9. CDFs of V_{sag} for each penetration level of the case # 2.

Fig. 10. CDFs of V_{sag} for each penetration level of the case # 3.

a result of higher PVDGs penetration. Finally, all the results obtained in this section are clearly consistent with the $SARFI_{x\%}$ indices previously calculated.

X. CONCLUSION

This paper proposed a method to assess the impacts of PVDG on the voltage sag indices of the LV systems considering loading condition based failure rates. The SEM was used with clustering techniques to model the irradiance uncertainty. An MCS with a more precise irradiance model was used to validate the proposed method. The SEM was used to estimate the variation of voltage sag indices with the growth of PVDG penetration using the condition dependence model and the constant failure rate model. The results showed that the contributions of PVDGs fault reduce the magnitudes of sags, but increase the duration, resulting in a general increase of moderate severity in relation to the SEMI

VTC. However, PVDGs reduced the frequency of sags due to the effect of reducing failure rates, relieving feeders loading. Consequently, there is a large reduction in the magnitude of the indices and a limitation in the growth of indices based on VTCs. Additionally, it was showed that the reduction in the sags frequency is the effect that caused higher impact due to the penetration of PVDGs in relation to the voltages sag indices. Finally, the proposed method was compared with a recently published method [9] and proved to be more accurate than it.

REFERENCES

[1] E. N. M. Silva, A. B. Rodrigues, and M. d. G. d. Silva, "Stochastic assessment of impact of photovoltaic distributed generation on the power quality indices of distribution networks," *Elect. Power Syst. Res.*, vol. 135, pp. 59–67, 2016.

[2] F. Shahnia, R. Majumderb, A. Ghosha, G. Ledwicha, and F. Zare, "Voltage imbalance analysis in residential low voltage distribution network with rooftop PVs," *Elect. Power Syst. Res.*, vol. 81, pp. 1805–1814, 2011.

[3] V. Hengristawat, T. Tayjasanant, and N. Nimpitiwan, "Optimal sizing of photovoltaic distributed generators in a distribution system with consideration of solar radiation and harmonic distortion," *Int. J. Elect. Power Energy Syst.*, vol. 39, pp. 36–47. 2012.

[4] R. C. Dugan, M. F. McGranaghan, S. Santoso, and H. W. Beaty, *Electrical Power Systems Quality*, 2nd ed. New York, NY, USA: McGraw-Hill, 2003.

[5] U. A. Bordalo, A. B. Rodrigues, and M. G. d. Silva, "A new methodology for probabilistic short-circuit evaluation with applications in power quality analysis," *IEEE Trans. Power Syst.*, vol. 21, no. 2, pp. 474–479, May 2006.

[6] J. C. Cebrian, J. V. Milanović, and N. Kagan, "Probabilistic assessment of financial losses in distribution network due to fault-induced process interruptions considering process immunity time," *IEEE Trans. Power Del.*, vol. 30, no. 3, pp. 1478–1486, Jun. 2015.

[7] J. E. R. Baptista, A. B. Rodrigues, and M. G. Silva, "Two probabilistic methods for voltage sag estimation in distribution systems," in *Proc. 19th Power Syst. Comput. Conf.*, Genoa, Italy, 2016, pp. 1–7.

[8] H. Liao, S. Abdelrahman, Y. Guo, and J. V. Milanović, "Identification of weak areas of power network based on exposure to voltage sags—part I: Development of sag severity index for single-event characterization," *IEEE Trans. Power Deliv.*, vol. 30, no. 6, pp. 2392–2400, Dec. 2015.

[9] S. Pukhrem, M. Basu, and M. Conlon, "Probabilistic risk assessment of power quality variations and events under temporal and spatial characteristic of increased pv integration in low voltage distribution network," *IEEE Trans. Power Syst.*, vol. 33, no. 3, pp. 3246–3254, May 2018.

[10] A. H. Etemadi and M. Fotuhi-Firuzabad, "Distribution system reliability enhancement using optimal capacitor placement," *IET Gener. Transmiss. Distib.*, vol. 2, no. 5, pp. 621–631, 2008.

[11] Y. Sun, P. Wang, L. Cheng, and H. Liu, "Operational reliability assessment of power systems considering condition-dependent failure rate," *IET Gener. Transmiss. Distrib.*, vol. 4, no. 1, pp. 60–72, 2010.

[12] M. Todorovski and D. Rajičić, "Handling three-winding tranformers and loads in short circuit analysis by the admittance summation method," *IEEE Trans. Power Syst.*, vol. 18, no. 3, pp. 993–1000, Aug. 2003.

[13] Task Force C6.04.02, "Benchmark systems for network integration of renewable and distributed energy," CIGRÈ, 2014.

[14] T. H. Chen, M. S. Chen, T. Inoue, P. Kotas, and E. A. Chebli, "Three-phase cogenerator and transformer models for distribution system analysis," *IEEE Trans. Power Deliv.*, vol. 6, no. 4, pp. 1671–1681, Oct. 1991.

[15] *Specification for Semiconductor Processing Equipment Voltage Sag Immunity*, SEMI International Standard F47-0706, 2006. [Online]. Available: http://www.semi.org.

[16] H. Hooshyar and M. E. Baran, "Fault analysis on distribution feeders with high penetration of PV systems," *IEEE Trans. Power Syst.*, vol. 28, no. 3, pp. 2890–2896, Aug. 2013.

[17] A. P. Moura, J. A. P. Lopes, A. A. F. d. Moura, J. Sumaili, and C. L. Moreira, "IMICV fault analysis method with multiple PV grid-connected inverters for distribution systems," *Elect. Power Syst. Res.*, vol. 119, pp. 119–125, 2015.

[18] J. C. Cebrian, N. Kagan, and J. V. Milanović, "Probabilistic estimation of distribution network performance with respect to voltage sags and interruptions considering network protection setting – part I: The methodology," *IEEE Trans. Power Del.*, vol. 33, no. 1, pp. 42–51, Feb. 2018.

[19] Instituto Nacional de Pesquisas Espaciais (INPE), "Sistema de Organização Nacional de Dados Ambientais (SONDA)," [Online]. Available: http://sonda.ccst.inpe.br. Accessed on: Jul. 2018.

[20] Y. M. Atwa, E. F. El-Saadany, M. M. A. Salama, and R. Seethapathy, "Optimal renewable resources mix for distribution system energy loss minimization," *IEEE Trans. Power Syst.*, vol. 25, no. 1, pp. 360–369, Feb. 2010.

[21] A. N. D. Tleiss, *Power System Modelling and Fault Analysis: Theory and Practice*. Oxford, U.K.: Elsevier, 2008.

[22] R. E. Brown, G. Frimpong, and H. L. Willis, "Failure rate modeling using equipment inspection data," *IEEE Trans. Power Syst.*, vol. 19, no. 2, pp. 782–787, May 2004.

João Eduardo Ribeiro Baptista received the B.Sc. and M.Sc. degrees in electrical engineering from the Federal University of Maranhão (UFMA), São Luís, Brazil, in 2014 and 2016, respectively. He is currently working toward the doctorate degree. He is a Lecturer with the UFMA. His main research interest includes probabilistic techniques applied to power quality assessment.

Anselmo Barbosa Rodrigues received the B.Sc. and M.Sc. degrees in electrical engineering from the Federal University of Maranhão (UFMA), São Luís, Brazil, in 1998 and 2003, respectively, and the D.Sc. degree in electrical engineering from the Pontifical Catholic University of Rio de Janeiro, Rio de Janeiro, Brazil, in 2009. He is an Assistant Professor with the Department of Electrical Engineering, UFMA. His research interests include power systems reliability, power quality, and probabilistic methods applied to power systems.

Maria da Guia da Silva received the B.Sc. and M.Sc. degrees in power engineering from the Federal University of Paraiba, Paraíba, Brazil, in 1980 and 1989, respectively, and the Ph.D. degree in power engineering from the Institute of Science and Technology, University of Manchester, Manchester, U.K., in 1994. She is an Associate Professor with the Department of Electrical Engineering, Federal University of Maranhao. Her primary research interests include power systems reliability, power quality, and probabilistic methods applied to power systems.